2007 IEEE International Conference on
Robotics and Automation
Roma, Italy, 10-14 April 2007

Recursive Measurement Process for Improving Accuracy of Dimensional Inspection of Automotive Body Parts

Quan Shi, Ning Xi, and Weihua Sheng

Abstract— **Accuracy is essential to surface quality control when a range sensor is applied to measure the 3D shape of an automotive body part. A sensor's viewing pose, including location and orientation, is related to measurement accuracy. It is usually difficult to find an optimal solution by manual control of sensor viewpoints. A CAD-guided robot view planner developed previously can automatically generate viewpoints. Measurement accuracy can be satisfied in a certain range. However, the unpredictable image noises, especially in regions with low intensity contrast, cannot be compensated by the CAD-guided robot view planner. In another aspect, measurement accuracy is evaluated all over the part surface. The local accuracy of a small patch may exceed the measurement tolerance. In this paper, feedback design is applied to the CAD-guided robot sensor planning system. The feedback controller can evaluate the accuracy of obtained point clouds, identify problem regions, and generate new viewpoints. This process is recursively executed until the measurement accuracy reaches to a tolerant value. This feedback-based inspection system had been implemented in previous work to fill holes of a point cloud, which are caused by shadows and light reflections. In this paper, the feedback controller is specifically designed to improve the measurement accuracy. Experimental results show the success of applying this feedback system for dimensional inspection of an automotive body part.**

I. INTRODUCTION

For quality control of a part's surface shape, a range sensor has many advantages than a traditional coordinate measurement machine (CMM). However, measurement accuracy has to be satisfied for industrial applications. Improving the design of a sensor itself, such as increasing the resolution of a camera/projector, can reduce measurement uncertainties. In another aspect, viewpoints of a range sensor, including the location and orientation, is also related to the accuracy of a 3D shape measurement [1][2]. It is often difficult to find an optimal solution by manually moving a range sensor to a proper viewpoint for obtaining a qualified point cloud. This problem is usually solved by a view planning system.

Many view planing systems [3][4] emphasize on minimizing the number of viewpoints and the length of paths. For shape inspection, a view planner should be designed to optimize the measurement accuracy as well. Furthermore, the priority of the accuracy need to be higher than the topology of the sensor path.

For an automatic vision-based 3D shape inspection system, measurement errors are inevitable and the sources of uncertainties usually include:

1) Intensity noise
2) Image quantization error
3) Poor surface property of light reflection.

Intensity noise is often a random noise in the process of counting photon energy for each pixel. This type of noise mainly depends on the image grabbing system and can be reduced by filtering techniques. The quantization error has been well studied [5][6]. The quantization error, unavoidable exists in almost all vision systems, is bounded by the size of pixels. A high resolution camera usually can provide better measurement accuracy. With a same camera, a proper viewpoint can also be used to reduce this quantization error [2]. Surface property of light reflection is a problem particularly when a projector is involved in a vision system. Because various materials have different reflection properties, the projected patterns may not be clearly recorded. For example, in a low contrast region of an image, error is often increased because the edge of projected fringes becomes easy to be noised.

A CAD-guided robot sensor planner is developed to generate an intelligent 3D shape inspection system [7]. It can effectively reduce the image quantization error by properly moving a range sensor. Optical constraints, such as field of view, pixel resolution, and focus distance, are integrated together to find a "best view" with the knowledge of a given CAD model. The image quantization error is constrained in a certain range under the planned viewpoints. However, when the bounding box method [7] is used to estimated viewpoints, average norm of triangles is adopted to determine viewpoint orientation. Therefore, for a small area in the planned view, measurement constraints may not be satisfied, which then increase the quantization error.

Feedback-based view planning method is a possible solution to improve measurement accuracy. A previous work had been developed to fill holes by solving the shadow and specular reflection problem [1]. In this paper, the feedback controller is design to find a better view to improve the collected image quality. Particularly, when a low contrast area is detected, new viewpoints will be generated to cover that part of surface. Although the processing time of this feedback-based system is much longer than a CAD-guided view planning system, the measurement accuracy will be improved, which is indeed required for industrial applica-

The work described in this paper is supported under NSF Grant IIS-9796300, IIS-9796287, EIA-9911077, DMI-0115355, and FORD Motor Company University Research Program.

Q. Shi is with the Department of Electrical and Computer Engineering, Michigan State University, East Lansing, MI. 48823, USA shiquan@egr.msu.edu

N. Xi is with Faculty of Electrical and Computer Engineering, Michigan State University, East Lansing, MI. 48823, USA xin@egr.msu.edu

W. Sheng is with Faculty of Electrical and Computer Engineering, Oklahoma State University, Stillwater, OK. 74078, USA weihua.sheng@okstate.edu

tions. The dynamic view planning system and the feedback controller is shown in Figure 1. Details of this feedback controller will be introduced in this paper.

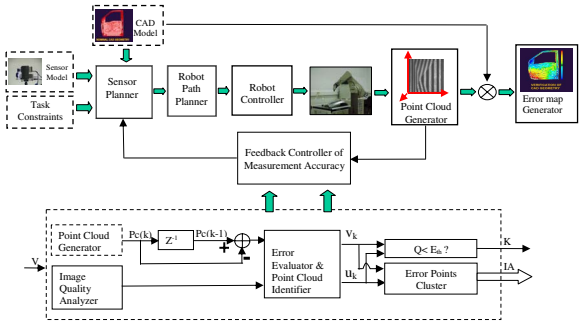

Fig. 1. A feedback-based robot sensor planning system for rapid 3D shape inspection

The goal of this dynamic planning process is not just to build an intelligent inspection system, our work more focus on improving the quality of the measured point clouds. which should be able to represent the true shape of a part. It also needs to point out, when additional viewpoints are added into a robot path, the density of the measured point cloud can also be increased, which optimize the point cloud quality in another aspect.

II. Analysis of Errors in 3D Shape Measurement

Stripes are used widely by many types of range sensors, precisely determining the boundaries of strips is a critical issue for a successful 3D shape measurement. A gray coded line shifting (GCLS) method had been applied to our digital light processor (DLP)-based range sensor [7]. To calculate the depth from one surface point to a pre-calibrated reference, edges of strips have to be calculated in sub-pixel resolution. If not, quantization error will be added into measurement results. As shown in Figure 2, the edge of a stripe can arbitrarily fall in anywhere between an image pixel n and its next pixel $n+1$.

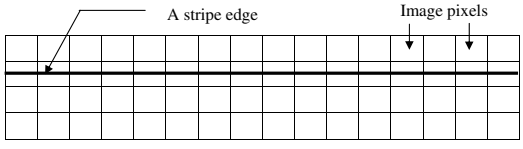

Fig. 2. Image quantization error in edge detection

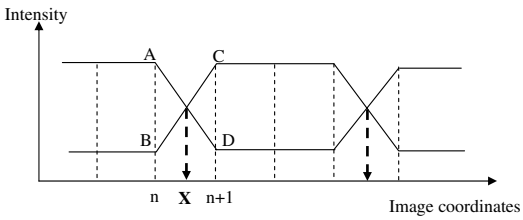

Fig. 3. Edge detection using interpolation strategy

An edge detection method is illustrated in Figure 3: using another image with opposite intensity stripes, A, B, C, and D represents four intensity values that will be used to calculate X, the location of a stripe boundary. Sub-pixel accuracy can be obtained with this interpolation calculation.

Even though, the estimation of X may have error because of image noises. But this error can be bounded in one image pixel. On a view surface that has a norm parallel to the viewing direction, resolution is often defined by the size of a piece surface projected onto one pixel. This resolution is a constraint widely used in many view planning system. For a freeform surface, it may contain many small patches, norms of each small patch will be vary so that the resolution of each patch is quite different. Average norm of all small patches, can be used to determines a viewpoint for those patches. This method only satisfies the global resolution constraint. However, for a small patch under that viewpoint, the angel between the surface norm and the viewing direction may exceed the threshold such that the resolution constraint cannot be satisfied. Hence, the one pixel error bound is increased and the measurement uncertainty will be out of tolerance. For surface shape inspection, this small area needs a new viewpoint to satisfy the measurement constraints.

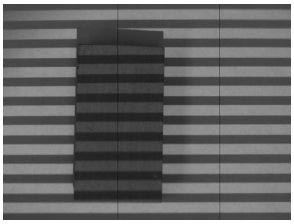

Fig. 4. An image of stripes in high/low contrast area

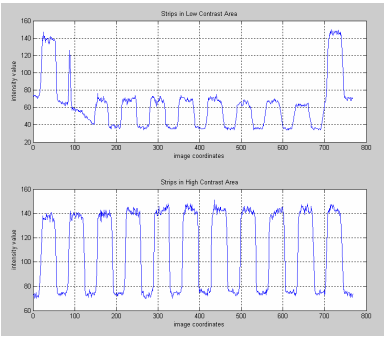

Fig. 5. Intensity profile in high/low contrast area

Besides quantization error, measurement uncertainty will also be increased in low contrast images. Considering intensity noises, stripes in a high contrast area will be more robust than stripes in a low contrast area. Figure 4 illustrates an image with high/low contrast regions. The intensity profiles of two lines in Figure 4 are displayed in Figure 5: the top curve shows the intensity profile of the line through a low contrast area and the bottom curve shows the intensity profile of another line through a high contrast area. Image noises can

be seen at the peak and valley of each wave, which affects the accuracy of the edge detection algorithm.

III. Mathematic Model of the Feedback-Based Inspection Process

The general framework of a feedback-based inspection process had been developed [1]. This feedback system has a CAD-guided sensor planner that can initially setup a set of viewpoints in the open-loop. A feedback controller was designed to add a set of viewpoints recursively according to the quality of the obtained point clouds. Holes generated by shadows and specular reflections were filled during the iteration process. After when the control system reach to the set point, a *complete* point cloud can be obtained for error map generation. The diagram of the whole feedback-based inspection system can be seen in Figure 6.

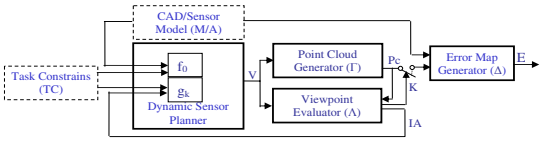

Fig. 6. Block diagram of a feedback-based dynamic shape inspection system

In this paper, the feedback controller is specially designed to improve the measurement accuracy. Mathematic model and stability of such a feedback system are all described in followings.

A. The model of system inputs, outputs, and functions

The dynamic sensor planner need various inputs such as CAD model and point cloud information. According to each type of input, viewpoints will generated and be added into a robot path. Except the range sensor model [7], the dynamic sensor planner has three more inputs: 1) CAD model, 2) task constraints, and 3) feedback information.

CAD model M is usually a group of triangles tessellated from part surfaces. Mathematically, it can be represented by:

$$M = \{T_i | T_i =< (X_{i1}, Y_{i1}, Z_{i1}), (X_{i2}, Y_{i2}, Z_{i2}), (X_{i3}, Y_{i3}, Z_{i3}) >, i = 1...n\} \quad (1)$$

Task constraints TC is a set of measurement requirements, which integrate the requirements for CAD-based planning strategy and feedback-based planning strategy:

$$TC = \{fov, S, \rho, f_d, \eta, \Sigma, \sigma\} \quad (2)$$

where the field of view fov is defined by the length L and width W of a rectangle area; S is the standoff distance of an area sensor; ρ represents the image resolution; f_d represents the focus distance which contains two values: nearest focus distance, and farthest focus distance; η represents visibility of the area sensor, determined by three vectors: projection vectors $\overrightarrow{PV}$, camera viewing vector $\overrightarrow{CV}$, and surface norm vector $\overrightarrow{SV}$. A piece of surface is visible if the following equation is satisfied:

$$\begin{cases} \arccos(\frac{\overrightarrow{PV}\cdot\overrightarrow{SV}}{||\overrightarrow{PV}\cdot\overrightarrow{SV}||}) < \theta_{th1} \\ \arccos(\frac{\overrightarrow{CV}\cdot\overrightarrow{SV}}{||\overrightarrow{CV}\cdot\overrightarrow{SV}||}) < \theta_{th2} \end{cases} \quad (3)$$

where θ_{th1} ensures that the encoded patterns can be projected onto the surface and θ_{th2} ensures that this piece of surface can be "seen" by camera. Σ represents the area of holes generated by shadows or light specular reflections. Stripes are totally lost in this part of area and the number of correspondent pixels are counted to determine the size of holes; σ is the standard deviation of measurement variations, calculated on same surfaces within two measurements. Ideally, the shape of those two point clouds should be identical. However, image quantization error and poor surface reflection property will increase the measurement uncertainties. Then, stand deviation of the differences of two measurements can be used to show how the two point clouds are vary from each other. If σ is larger than a predetermined threshold, another viewpoint then need to be set for this area.

Feedback information contains the analysis results of the measured point clouds, which are usually three types of defect map: a shadow map IS, a reflection map IR, and an inaccuracy map IA [1]. The shadow map and reflection map have been described previously, in this paper, we focuses on the inaccuracy map IA, which is described in Equation 4, p_i represents a 3D point in a region which has quite different shape between two measurements, ka represents the number of points in this region, and σ_{th} is a threshold value predefined as the requirement of measurement accuracy.

$$IA = \{p_i(x_{ai}, y_{ai}, z_{ai}) | i = 1, 2...ka, \sigma > \sigma_{th}\} \quad (4)$$

Measurement error is not evenly distributed over a point cloud [7]. For a single surface point, the measurement accuracy is related to the sensor viewpoint. The accuracy map IA can effectively show the differences between the measurements on two viewpoints.

Viewpoints are the output of this dynamic sensor planner. A viewpoint includes a location p and a viewing vector v. As shown in Equation 6, V_0 represents the initial set of viewpoints generated from CAD model, V_k represents the sets of viewpoints estimated in feedback, k represents the iteration times.

$$\begin{aligned} V_0 &= \{\Psi_{0i} = (p_i, v_i), p_i \in R^3, v_i \in R^3\} \\ V_k &= \{\Psi_{ki} = (p_{ki}, v_{ki}), p_{ki} \in R^3, v_{ki} \in R^3\} \\ V &= (\bigcup_{k=1}^{n} V_k) \bigcup V_0 \end{aligned} \quad (5)$$

The developed dynamic sensor planner also has two functions:

1) Initial viewpoint configuration f_0: An initial viewpoint configuration is a process to estimate viewpoints based on the given CAD model of a part. Function f_0

represents a bounding box algorithm developed to find a viewpoint set V_0 from CAD model M.

$$f_0 : M \mapsto V_0 \tag{6}$$

2) Feedback-based viewpoint configuration g_k: g_k is a projection from a defect map IA to new viewpoints.

$$g_k : IA \mapsto V_k \tag{7}$$

The viewpoint evaluator Λ is a function, which makes a decision about if the quality of a point cloud Pc satisfies the measurement requirement. If not, defect map IA will be fed back to the dynamic sensor planner to update set V.

$$\Lambda : V \mapsto IA \tag{8}$$

where viewpoint set V is the input to Λ. Figure 7 illustrates

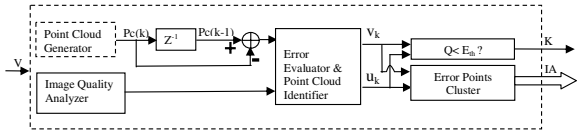

Fig. 7. Block diagram of the feedback controller, viewpoint evaluator Λ

the detail structure of this function. Two point clouds will be measured sequentially. Differences between those two point clouds will be input to the error evaluator. Meanwhile, an image processor is designed to identify the area with intolerant shape differences. Symbol u_k and v_k are used for system stability analysis and will be described next. A logic switch signal K is the output signal of Λ. Q is a cost function that determine the area of inaccurate points. If Q is less than a threshold E_{th}, the switch k will be closed and the iteration process will be stopped, the current point cloud can then be sent out for comparison with its CAD model M.

The mathematic models of a point cloud Pc, a point cloud generator Γ and an error map generator Δ, shown in Figure 6 have been introduced in details in [1].

B. The model of the dynamic measurement process

Equation (9) describes the model of the dynamic view planning process in a state space: V and Pc are state variables, M and TC are inputs, and error map E is the output of the system:

$$\begin{cases} V & \doteq f_0(M,TC) \cup g_k(IA) \\ Pc & \doteq \Gamma(V) \\ E & = \Delta(M,Pc) \end{cases} \tag{9}$$

where $\doteq$ indicates that V and Pc are accumulated results from iterations. As shown in Figure 6, given a CAD model M and a set of task constraints TC, a group of viewpoints V_0 will be initialized first, a point cloud Pc is then generated according to V_0. Initially, V is equal to V_0. Two functions Γ and Λ are then going to be executed based on this viewpoint set V. As described previously, Γ is an execution to obtain point clouds Pc from set V. Meanwhile, function Λ evaluates the current viewpoint by detecting regions of inaccurate points. If necessary, a group of new viewpoints can then be generated through function g_k. The measured point cloud is kept updating until the cost function Q reports a stop signal. According to this automatic control scheme, an error map can be generated only when the measured point cloud is considered to be accurate. This final point cloud will be used for surface quality inspection.

C. Stability analysis of the feedback controller

Stability of this dynamic inspection process is analyzed to ensure the iteration process will converge. As described above, a cost function Q is used to determine when the feedback will stop, generally, Q is calculated according to the area of holes and the area of inaccurate measurements. Seen in Equation (10), u represents the total area of holes, called a hole cost. And v represents the total area of shape difference between two point clouds, called a distance cost. Then, Q can be optimized by adding more viewpoints such that both u and v are minimized. The cost function Q can be represented on a complex plane such that u and v are the real and imaginary part respectively. A weight number w is defined as a ratio between the hole cost and the distance cost. For filling holes, the v can be set to "0" because the hole cost is going to be focused. Similarly, when focusing on viewpoints to improve the measurement accuracy, u can be ignored at this time. In combination of hole and accuracy, w can be set to a number from "0" to "10", depends on the number of holes and the size of each hole. If only several small holes include, w is set to a value less than "1", but if a big hole is detected, w then need to be set to a large number close to "10".

$$Q = \|w \cdot u_k + j v_k\| \tag{10}$$

The recursive planning process stops when Q is reduced to a tolerant value. Ideally, Q would be 0, indicating that the present point cloud has no holes and is exactly identical to the point cloud measured in last step. Because new viewpoints will always bring more 3D points to update the point cloud, the hole cost and the distance cost could be minimized by continuously adding viewpoints. Hence, the system will be stable after a finite number of iterations, k.

IV. Experimental Implementation and Results

An accuracy test is conducted first on flat surface with difference intensity contrast property. Figure 8 shows the deviations of measurements: Figure 8(a) displays the result in low contrast region and Figure 8(b) displays the result in high contrast region. It can be seen that the deviation of measurements in the high contrast region is smaller than it in the low contrast region.

A method to solve this problem is to move the range sensor close to the low contrast surface region and take multiple measurements on that viewpoint. Collecting and averaging the point cloud data from multiple measurements can effectively reduce the measurement error. Results of a test on a flat surface are shown in Figure 9, in which (a) shows the deviation of the measured surface from a single shot and

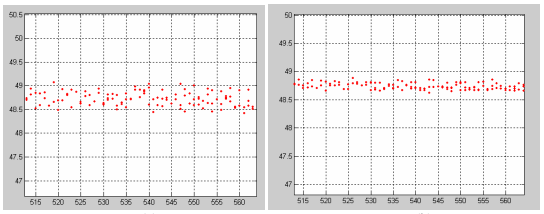

Fig. 8. Deviation of measurement errors. (a) Deviation of results in a low contrast region (b) Deviation of results in a high contrast region

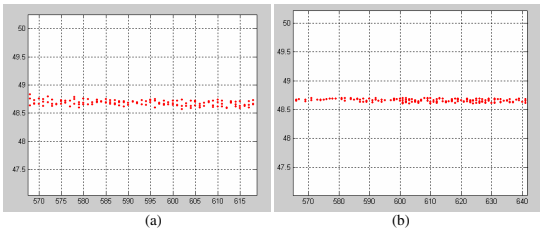

Fig. 9. Reduce measurement uncertainty in a low contrast area by replacing the range sensor and averaging data from multiple measurements. (a) Deviation of results on a viewpoint close to surface with single shot (b) Deviation of results on a viewpoint close to surface with multiple shots

(b) shows the average height calculated from multiple shots. Meanwhile, compare Figure 9 (a) to Figure 8(a), it can be seen that the deviation becomes smaller when the sensor is close to the part surface. The trade off of this method is, more calculations have to be executed for measuring this surface, such as the identification of low contrast region, planning new viewpoints, and data processing of 3D shape measurements.

The developed dynamic inspection system has been implemented on a PUMA 560 robot. An automotive body part, pillar-m32510, is used for system testing. Viewpoints can be simulated using $NuGraf^{TM}$. Detailed information about system setup has been described in [7].

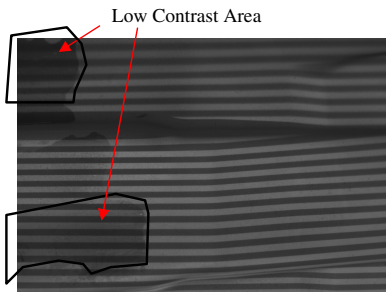

Fig. 10. Measurement of part surface with low intensity contrast areas

Figure 10 shows the collected images of stripes within high/low contrast regions. The low contrast region can be detected using image processing technique, measurement results show that the uncertainties are not tolerant in this region. Another viewpoint is generated accordingly using the feedback information. The iteration process is conducted ten times, the standard deviation of points all over the point cloud are calculated. The variation of the obtained point clouds

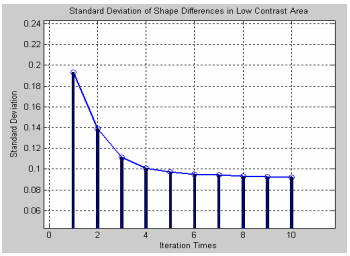

Fig. 11. Stability analysis of the feedback system

becomes smaller and smaller, and the feedback process is going to stop at when the cost function(per) δ reaches to a predetermined set point.

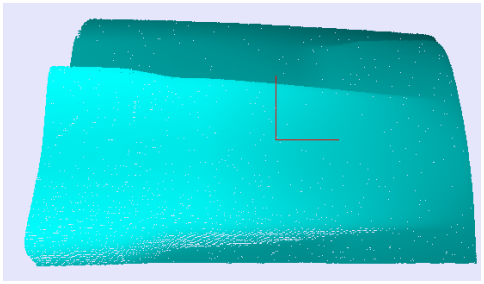

Fig. 12. A measured point cloud after iterations

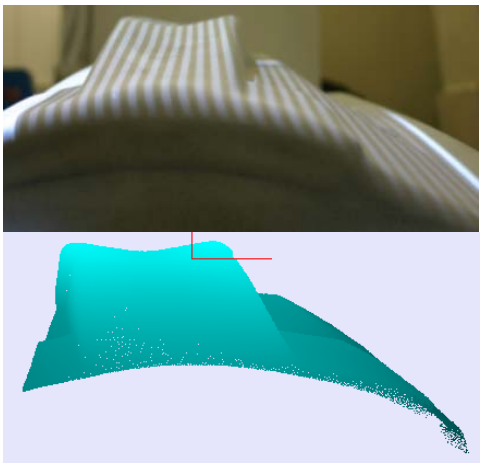

Fig. 13. Stripes and the correspondent point cloud from another view

The curve of the standard deviation between two point clouds is shown in Figure 11. The number is dropped from 0.1981 to 0.0921 at the last step. The point cloud obtained in the last step is shown in Figure 12. Figure 13 displays the 3D part surface and its correspondent point cloud from another view.

Table I shows the results of each iterations. With more points are obtained in each step, the standard deviation of shape differences between each two measurements are reduced as well as the cost to evaluate the quality of the point cloud. This recursive process stops when the cost is less than a predefined limit 0.025.

TABLE I

IMPROVE ACCURACY FROM A RECURSIVE PROCESS

Iterations, k	σ	time, t(sec)	No. of Points	cost
k=1	0.1934	41.2	243,185	0.1718
k=2	0.1387	72.0	363,348	0.1021
k=3	0.1113	101.0	356,734	0.0602
k=4	0.1011	130.4	365,343	0.0450
k=5	0.0975	159.4	375,239	0.0378
k=6	0.0951	178.6	364,347	0.0329
k=7	0.0944	207.9	353,283	0.0280
k=8	0.0931	238.1	345,342	0.0265
k=9	0.0928	267.7	364,812	0.0253
k=10	0.0921	295.3	345,453	0.0249

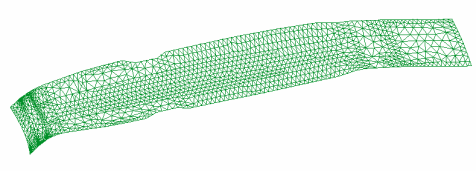

Fig. 14. CAD model of an automotive body part,

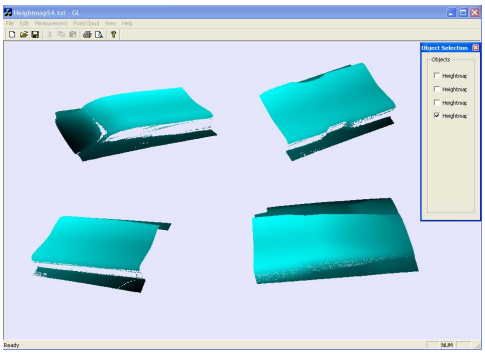

Fig. 15. Point Clouds of pillar-m32510, measured from four viewpoints

Figure 14 displays a tessellated CAD model of an automotive body part, pillar-m32510. There are totally 2,716 triangles used to represent the geometry shape of this part. The measured point clouds are shown in Figure 16. The measured point clouds can be registered together to form a point cloud, which represents the geometry shape of the real part.

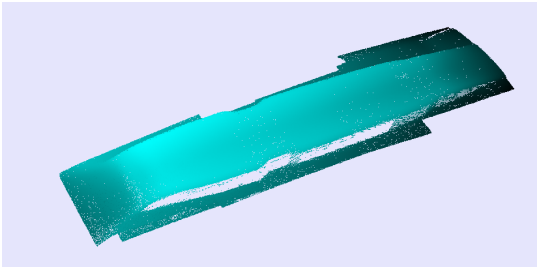

Fig. 16. The entire point cloud of part pillar-m32510

Shape difference between the CAD model and the registered point cloud can be illustrated by a color-coded error map. As shown in Figure 17: at the left side of part, the surface is higher than the designed shape. The reason is that

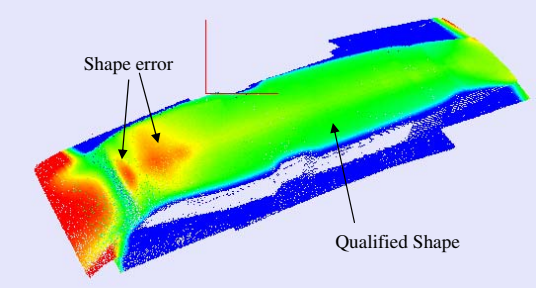

Fig. 17. A color-coded error map of part pillar-m32510

this part is punched under pressure, because the curvature is not that smooth as the right side, forces are not only from the top but also from the left, push the surface up than it supposed to be. This part of area need to be checked again in manufacturing process to ensure that shape of this part meets the dimensional requirements.

V. CONCLUSIONS

A feedback-based robot view planning system is developed to improve the accuracy of a 3D shape measurement. Image quantization error and poor surface property will increase the measurement uncertainties. Dynamic sensor planning methods are developed in a feedback-based planning system to improve the measurement quality. The developed system can recursively add new viewpoints for 3D shape measurement. The feedback process will stop when the quality of point clouds are satisfied for error map generation. Mathematical model of this system are developed. An application of this feedback-based planning system is shown in an experiment on an automotive body part.

REFERENCES

[1] Q. Shi, N. Xi, W. Sheng, and Y. Chen, *Development of Dynamic Inspection Methods for Dimensional Measurement of Automotive Body Parts*, IEEE International Conference on Robotics and Automation, Accepted, 2006.

[2] C. C. Yang, M. M. Marefat, and F. W. Ciarallo, *Error analysis and planning accuracy for dimensinal measurement in active vision inspection*, IEEE Transactions on Robotics and Automation, Vol. 14, NO. 3 June 1998.

[3] W. R. Scott, G. Roth, J. F. Rivest, *View Planning for Automated Three-Dimensional Object Reconstruction and Inspection*, ACM Computing Surveys, Vol. 35, No. 1, pp. 64-96, 2003.

[4] M. Angel Garcia, S. Velazquez, A. Domingo Sappa, and L. Basanez, *Autonomous Sensor Planning for 3D Reconstruction of Complex Objects from Range Images*, IEEE International Conference on Robotics and Automation, Leuven, Belgium, pp. 3085-3090, May, 1998.

[5] B. Kamgar-Parsi and B. Kamgar-Parsi, *Evaluation of quantization error in computer vision* IEEE Transactions on Pattern Analysis and Machine Intelligence, vol. 11, Sept. 1989.

[6] S. D. Blostein and T. S. Huang, *Error analysis in stereo determination of 3-D point positions* IEEE Transactions on Pattern Analysis and Machine Intelligence, vol. 9, Nov, 1987.

[7] Q. Shi, N. Xi, H. Chen, Y. Chen, *Integrated Process for Measurement of Free-Form Automotive Part Surface Using a Digital Area Sensor*, IEEE International Conference on Robotics and Automation, pp. 580-585, 2005.